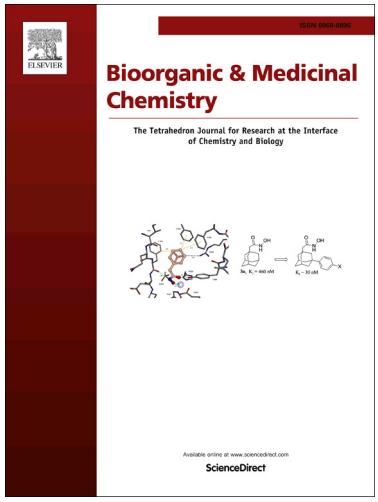

Synthesis of novel triazoles and a tetrazole of escitalopram as cholinesterase inhibitors

Mehr-un-Nisa, Munawar A. Munawar, Fauzia A. Chattha, Samina Kousar, Jawaria Munir, Tayaba Ismail, Muhammad Ashraf, Misbahul A. Khan

PII: S0968-0896(15)00545-3
DOI: http://dx.doi.org/10.1016/j.bmc.2015.06.051
Reference: BMC 12407

To appear in: *Bioorganic & Medicinal Chemistry*

Received Date: 9 May 2015
Revised Date: 17 June 2015
Accepted Date: 18 June 2015

Please cite this article as: Mehr-un-Nisa, Munawar, M.A., Chattha, F.A., Kousar, S., Munir, J., Ismail, T., Ashraf, M., Khan, M.A., Synthesis of novel triazoles and a tetrazole of escitalopram as cholinesterase inhibitors, *Bioorganic & Medicinal Chemistry* (2015), doi: http://dx.doi.org/10.1016/j.bmc.2015.06.051

Graphical Abstract.

Synthesis of novel triazoles and a tetrazole of escitalopram as cholinesterase inhibitors

Mehr-un-Nisa [a] , Munawar A. Munawar [a,] *, Fauzia A. Chattha [a], Samina Kousar [a], Jawaria Munir [a,d], Tayaba Ismail [c], Muhammad Ashraf [b] and Misbahul A. Khan [a,b].

[a] *Institute of Chemistry, University of the Punjab, Lahore-54590, Pakistan*
[b] *Department of Chemistry, The Islamia University of Bahawalpur, Bahawalpur-63100, Pakistan*
[c] *Department of Biochemistry & Biotechnology, The Islamia University of Bahawalpur, Bahawalpur-63100, Pakistan*
[d] *Institute of Molecular Sciences & Bioinformatics, Lahore-54000, Pakistan*

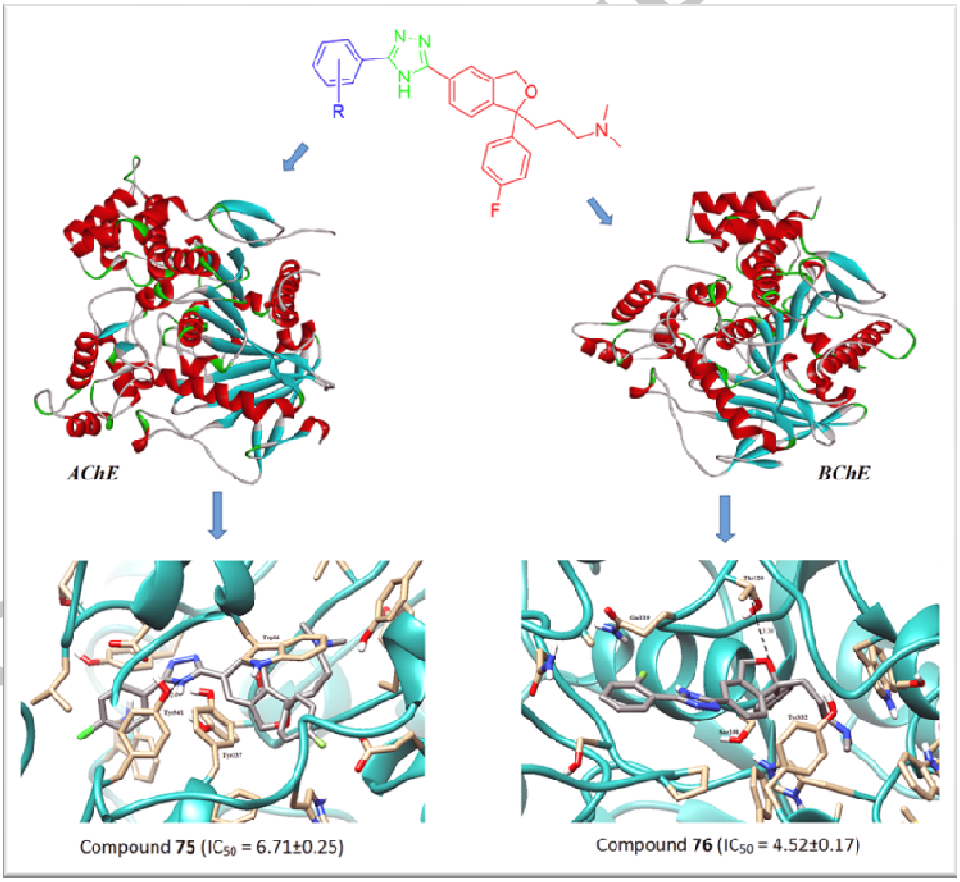

Bioorganic & Medicinal Chemistry
journal homepage: www.elsevier.com

Synthesis of novel triazoles and a tetrazole of escitalopram as cholinesterase inhibitors

Mehr-un-Nisa [a], Munawar A. Munawar [a,*], Fauzia A. Chattha [a], Samina Kousar [a], Jawaria Munir [a,d], Tayaba Ismail [c], Muhammad Ashraf [b] and Misbahul A. Khan [a,b].

[a] *Institute of Chemistry, University of the Punjab, Lahore-54590, Pakistan*
[b] *Department of Chemistry, The Islamia University of Bahawalpur, Bahawalpur-63100, Pakistan*
[c] *Department of Biochemistry & Biotechnology, The Islamia University of Bahawalpur, Bahawalpur-63100, Pakistan*
[d] *Institute of Molecular Sciences & Bioinformatics, Lahore-54000, Pakistan*

ARTICLE INFO

Article history:
Received 09 May 2015
Received in revised form
Accepted
Available online

Keywords:
Acetylcholinesterase,
butyrylcholinesterase,
escitalopram,
triazoles,
cholinesterase

ABSTRACT

A novel serie of escitalopram triazoles (**60-88**) and a tetrazole (**89**) have been synthesized and subjected to a study to establish the inhibitory potential of these compounds toward acetylcholinesterase (AChE) and butyrylcholinesterase (BChE). Some selectivity in inhibition has been observed. The 4-chlorophenyl- (**75,** IC_{50}, 6.71±0.25 μM) and 2-methylphenyl- (**70,** IC_{50}, 9.52±0.23 μM) escitalopram triazole derivatives depicted high AChE inhibition, while 2-fluorophenyl- (**76**, IC_{50} = 4.52±0.17 μM) and 4-fluorophenyl- (**78**, IC_{50} = 5.31±0.43 μM) have found to be excellent BChE inhibitors. It has also been observed that *ortho*, *meta* and *para* substituted electron donating groups increase the inhibition, while electron withdrawing groups reduce the inhibition. Docking analyses of inhibitors with AChE have depicted the binding energies for **70** and **75** as ΔG_{bind} -6.42 and -6.93 kcal/mol respectively, while ligands **76** and **78** have shown the binding affinity ΔG_{bind} -9.04 and -8.51 kcal/mol respectively for BChE.

1. Introduction

Acetylcholinesterase Acetylcholinesterase (AChE) hydrolyzes acetylcholine quicker as compared to other esterases and is the target of various potent toxins comprising snake venom, insecticides and chemical weapons[1]. AChE enzyme is located in high concentration in all kinds of central and peripheral tissues, conducting tissues, nerves and muscles, motor and sensory fibres, sympathetic and parasympathetic so called cholinergic and non-cholinergic fibres and also in areas where cell bodies and junctions are present. It plays an important role in cholinergic neurotransmission and quickly hydrolyses the neurotransmitter acetylcholine (Ach) into choline and acetate[2]. AChE has been found to be directly related to various neuromuscular disorders *e.g.,* glaucoma, myasthenia gravis[3], and to relieve the cholinergic deficiency associated with Alzheimer disease[4,5]. *In vivo* and *in vitro* studies in the CNS have indicated that developmentally regulated AChE plays a vital role in morphometric processes, cell differentiation, synaptogenesis along nervous system, and in neurite growth[6, 7]. Certain evidences have been found for its role in the hydrolysis of Met- and Leu-enkephalines and substance P, in degradation of other neuropeptides[8, 9] and in heart morphogenesis[10, 11].

BChE also named as pseudocholinesterase and plasma cholinesterase, is a non-specific cholinesterase enzyme that hydrolyses various choline esters[12]. In humans, it is located mainly in liver[12] and is encoded by the BChE gene[13]. The BChE function has not been fully elucidated; however, it scavenges anti-cholinesterase agents and defends synaptic AChE from inhibition. BChE has been explored as a possible stoichiometric bioscavenger in organophosphorus nerve agent poisoning[14-16]. It is extensively dispersed in the mammal's nervous system, indicating participation in the neural functions and in neurodegenerative diseases[17]. Its deficiency results in delayed

Abbreviations: AcOH, acetic acid; Ach, acetylcholine; AChE, acetylcholinesterase; ASCh, acetylthiocholine; BChE or BuChE, butyrylcholinesterase; BSCh, butyrylthiocholine; CNS, central nervous system; DMF, *N,N*-dimethylformamide; DMSO, dimethylsulfoxide; DTNB, 5,5'-Dithiobis-(2-nitrobenzoic acid), Ellman's reagent; MOE, molecular operating environment; NMR, nuclear magnetic resonance spectroscopy; ppm, parts per million; RCSB, the research collaboratory for structural bioinformatics; SAR, structure-activity relationship; NaN_3, sodium azide; TLC, thin layer chromatography.

* Corresponding author. Tel.: +92-300-4392363; fax: +92-42-99230998; e-mail: mamunawar.chem@pu.edu.pk

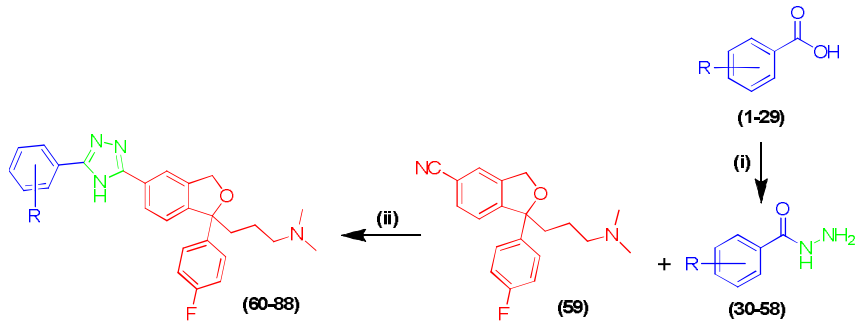

1, 30, 60 (R = H), **2, 31, 61** (R = 2-NH_2), **3, 32, 62** (R = 3-NH_2), **4, 33, 63** (R = 4-NH_2),
5, 34, 64 (R = 2-OH), **6, 35, 65** (R = 3-OH), **7, 36, 66** (R = 4-OH), **8, 37, 67** (R = 2-NO_2),
9, 38, 68 (R = 3-NO_2), **10, 39, 69** (R = 4-NO_2), **11, 40, 70** (R = 2-CH_3), **12, 41, 71** (R = 3-CH_3),
13, 42, 72 (R = 4-CH_3), **14, 43, 73** (R = 2-Cl), **15, 44, 74** (R = 3-Cl), **16, 45, 75** (R = 4-Cl),
17, 46, 76 (R = 2-F), **18, 47, 77** (R = 3-F), **19, 48, 78** (R = 4-F), **20, 49, 79** (R = 2-Br),
21, 50, 80 (R = 3-Br), **22, 51, 81** (R = 4-Br), **23, 52, 82** (R = 2-I), **24, 53, 83** (R = 3-I),
25, 54, 84 (R = 4-I), **26, 55, 85** (R = 2-OCH_3), **27, 56, 86** (R = 3-OCH_3), **28, 57, 87** (R = 4-OCH_3),
29, 58, 88 (R = 4-OH-3-OCH_3)

Scheme 1. Synthetic route of escitalopram triazoles (**60-88**). Reagents and conditions: (i) C_2H_5OH, 3N H_2SO_4, reflux, 6 h, $NaHCO_3$, $N_2H_4.H_2O$, AcOH reflux, 3-6 h (ii) n-butanol, K_2CO_3, reflux, 4-5 h.

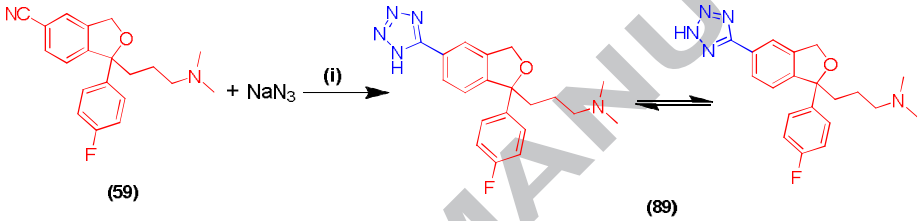

Scheme 2. Synthetic route of escitalopram tetrazole (**89**). Reagents and conditions: (i) DMF, NH_4Cl

metabolism of certain compounds *e.g.*, succinylcholine, mivacurium, heroin, procaine and cocaine. The depolarizing neuromuscular blocker, succinylcholine has been claimed to be hydrolyzed to succinylmonocholine and than succinic acid by BChE[18].

The development of new and safe clinically important therapeutic agents has been one of the main targets of pharmaceutical chemists. The success of imidazole as an important moiety of a number of medicinal agents led to introduction of the triazoles. The triazoles are said to be the isosteres of imidazoles in which the carbon atom of imidazole is isosterically replaced by nitrogen[19]. Triazole nucleus has been introduced into a wide range of therapeutically interesting drug candidates including CNS stimulants, anti-inflammatory, anti-anxiety, sedatives and antimicrobial agents, antifungal agents[20].

Citalopram is an anti-depressant of the selective serotonin reuptake inhibitor (SSRI) class. Preliminary facts from imaging studies[21] propose that Alzheimer's disease (AD) patients treated with galantamine may have further improvement in cerebral blood flow when also treated with citalopram. It has also been reported that clinical advantage from joint galantamine and citalopram may be associated to a synergistic inhibition of BuChE, assisting cholinergic neurotransmission.[22]

Herein, we have designed and synthesized a series of triazoles (**60-88**) and a tetrazole (**89**) conjugates of escitalopram (a selective serotonin reuptake inhibitor) and have checked for their potential role in the inhibition of AChE and BChE activities

2. Results and Discussion

2.1. Design

1,2,4-Triazoles occupied a unique position in heterocyclic chemistry due to its diverse biological significances *e.g.,* antimicrobial, anti-inflammatory, hypoglycemic, antidepressant, antitubercular, analgesic, anti-malarial and anticancer agents[20,23]. Escitalopram (**59**) is a selective serotonin reuptake inhibitor and very effective in depression, migraine, schizophrenia *etc*. In the present study, the escitalopram (**59**) has been converted into triazoles (**60-88**) and tetrazole (**89**) by reacting with benzohydrazides (**30-58**) and sodium azide respectively. The synthesized compounds (**60-89**) have been screened against AChE and BChE enzymes.

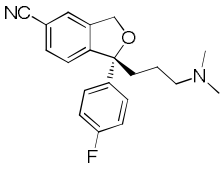

(**59,** Escitalopram)

2.1. Chemistry

Benzoic acid and its derivatives (**1-29**) were converted into benzohydrazides (**30-58**) by one pot conventional method[24]. The 1,2,4-triazoles (**60-88**) from escitalopram (**59**) were synthesized by adopting a reported method which involve the heating of benzohydrazide (**30-58**), escitalopram (**59-**oxalate) and K_2CO_3 mixture in n-butanol at 150 ^oC for 5-6 hours (Scheme 1)[25]. The triazole products (**60-88**) were purified first with column and then preparative thin layer chromatography.

Tetrazole of escitalopram (**89**) was synthesized by following a reported method (Scheme 2)[26] Escitalopram (**59-**oxalate), sodium azide and ammonium chloride were dissolved in DMF and heated on an oil bath for 7 hours at 125 ^oC. The tetrazole (**89**) was purified using column chromatography and finally RP-

Table 1. Determination of IC_{50} values of AChE of escitalopram triazoles and tetrazole.

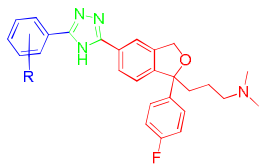

Compd. No.	-R	Conc. mM	AChE % Inhibition	AChE IC_{50} (μM)[a]	Compd. No.	-R	Conc. mM	AChE % Inhibition	AChE IC_{50} (μM)[a]
60	H	0.5	30.38±0.82	> 500	75	4-Cl	0.5	91.61±0.71	6.71±0.25
61	2-NH_2	0.5	70.19±0.96	359.72±0.34	76	2-F	0.25	62.12±0.13	187.51±0.16
62	3-NH_2	0.5	29.94±0.95	> 500	77	3-F	0.5	32.18±0.25	< 500
63	4-NH_2	0.5	15.32±0.85	-	78	4-F	0.5	71.55±0.86	260.63±0.29
64	2-OH	0.5	16.27±0.21	-	79	2-Br	0.5	19.43±0.91	-
65	3-OH	0.25	39.27±0.15	< 500	80	3-Br	0.5	37.91±0.73	< 500
66	4-OH	0.5	59.18±0.59	387.56±0.23	81	4-Br	0.5	15.63±1.12	-
67	2-NO_2	0.5	5.09±0.76	-	82	2-I	0.5	72.34±0.87	310.31±0.28
68	3-NO_2	0.5	81.65±0.76	138.23±0.17	83	3-I	0.5	25.06±0.53	> 500
69	4-NO_2	0.5	16.23±0.56	-	84	4-I	0.5	30.51±0.67	> 500
70	2-CH_3	0.5	88.64±0.84	9.52±0.23	85	2-OCH_3	0.5	80.44±1.19	161.34±0.49
71	3-CH_3	0.5	88.07±0.12	133.23±0.24	86	3-OCH_3	0.5	89.65±0.76	123.77±0.32
72	4-CH_3	0.5	16.01±0.51	-	87	4-OCH_3	0.5	10.35±0.97	-
73	2-Cl	0.5	19.46±0.16	-	88	4-OH-3-OCH_3	0.5	34.78±0.41	< 500
74	3-Cl	0.5	57.41±0.98	412.56±0.45	89	Tetrazole	0.5	70.58±0.37	251.67±0.14
Eserine Std.		0.5	91.27±1.17	0.04±0.0001					

[a]Results are the mean of three independent experiments (n = 3) ± S.D.

HPLC. The synthesized compounds were characterized by ^{1}H NMR, ^{13}C NMR, HRMS and Low Resolution Mass Spectrometry.

2.3. Biological Evaluation

The biological activities of the novel escitalopram triazoles (**60-88**) and a tetrazole (**89**) toward cholinesterase were evaluated using Ellman method. Eserine was used as positive control.

The evaluation of the activity of cholinesterase inhibitors by this method is based on the fact that AChE/BChE interacts with the inhibitor, and avoiding the acetyl/butyrylcholine hydrolysis. The inhibitor minimizes the enzyme activity which depends on the inhibitor concentration. The unbound enzyme can hydrolyze the added acetyl/butyrylthiocholine (ASCh/BSCh) whose amount is measured indirectly, by quantification of the product of its reaction with DTNB (5,5′-dithiobis-(2-nitrobenzoic acid)). Ellman method depends on the spectrophotometric quantification of the product of the reaction with DTNB.

2.3.1. AChE Inhibition

In the present study, a series of synthesized triazoles (**60-88**) and tetrazole (**89**) of escitalopram have been tested for AChE inhibition activities (Table 1). The inhibition pattern of this series against found to be 4-Cl>2-CH_3>3-OCH_3>3-CH_3>3-NO_2>2-OCH_3>2-F. The studies show that 4-chloro- (**75**, IC_{50}, 6.71±0.25 μM) and 2-methyl- (**70**, IC_{50}, 9.52±0.23 μM) are the most active compounds against AChE. The five compounds 3-NO_2- (**68**), 3-CH_3- (**71**), 2-F- (**76**), 2-OCH_3- (**85**) and 3-OCH_3- (**86**) have depicted moderate enzyme inhibitions with IC_{50} values ≤ 200 μM) with the following of order of decreasing activity as 3-OCH_3>3-CH_3>3-NO_2>2-OCH_3>2-F (Table 1).

Other compounds 2-aminophenyl- (**61**), 3-hydroxyphenyl- (**65**), 4-hydroxyphenyl- (**66**), 3-chlorophenyl- (**74**), 4- fluorophenyl- (**78**), 3-bromophenyl- (**80**), 2-iodophenyl- (**82**), 4-hydroxy-3-methoxyphenyl- (**88**) of the triazole series and tetrazole- (**89**) have demonstrated weak inhibitions (Table 1).

It's worth noting that mild electron donating groups enhance the AChE inhibition. However, the size and the position of the substituents also matter. In *ortho* substituted ligands, the observed order of their activity has been found as follow 2-CH_3>2-OCH_3>2-F>2-I>2-NH_2. Similarly, among the *meta* substituted ligands, 3-OCH_3 (**86**) has shown more inhibition of AChE as compared to 3-CH_3 (**71**). Among *para* substituted

Table 2. Determination of IC_{50} values of BChE of escitalopram triazoles and tetrazole.

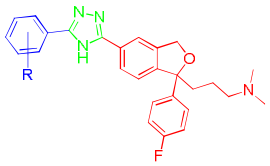

Compd. No.	-R	Conc. mM	BChE		Selectivity for BChE[b]	Compd. No.	-R	Conc. mM	BChE		Selectivity for BChE[b]
			% Inhibition	IC_{50} (μM)[a]					% Inhibition	IC_{50} (μM)[a]	
60	H	0.5	81.76±0.76	128.74±0.19	>3.88	75	4-Cl	0.5	73.68±0.36	151.35±0.23	0.044
61	2-NH_2	0.5	71.66±0.82	110.53±0.11	3.25	76	2-F	0.25	93.61±0.76	4.52±0.17	41.48
62	3-NH_2	0.5	73.55±0.88	187.54±0.11	>2.67	77	3-F	0.5	82.87±0.98	44.83±0.35	<11.15
63	4-NH_2	0.5	72.11±0.91	119.21±0.34	-	78	4-F	0.5	92.51±0.89	5.31±0.43	49.08
64	2-OH	0.5	80.71±0.63	101.52±0.27	-	79	2-Br	0.5	75.03±0.63	140.93±0.16	-
65	3-OH	0.25	61.66±0.71	118.54±0.31	<4.22	80	3-Br	0.5	85.45±0.85	78.02±0.39	<6.41
66	4-OH	0.5	78.66±0.85	140.22±0.29	2.76	81	4-Br	0.5	50.58±0.57	491.73±0.32	-
67	2-NO_2	0.5	62.87±0.49	296.53±0.25	-	82	2-I	0.5	84.50±0.93	25.91±0.27	11.98
68	3-NO_2	0.5	79.16±0.62	105.23±0.18	1.32	83	3-I	0.5	75.45±0.83	187.54±0.18	>2.67
69	4-NO_2	0.5	69.66±0.69	106.41±0.36	-	84	4-I	0.5	85.63±0.98	160.95±0.33	>3.11
70	2-CH_3	0.5	85.03±0.96	99.74±0.32	0.095	85	2-OCH_3	0.5	-2.13±0.15	-	-
71	3-CH_3	0.5	71.51±0.87	89.24±0.28	1.49	86	3-OCH_3	0.5	91.03±0.97	103.43±0.12	1.20
72	4-CH_3	0.5	91.05±0.89	151.87±0.34	-	87	4-OCH_3	0.5	81.21±0.87	167.82±0.37	-
73	2-Cl	0.5	79.63±0.52	81.41±0.21	-	88	4-OH-3-OCH_3	0.5	88.61±1.13	24.10±0.39	<20.75
74	3-Cl	0.5	79.92±1.11	26.53±0.58	15.73	89	Tetrazole	0.5	81.82±0.37	75.89±0.14	3.32
Eserine Std.		0.5	82.82±1.09	0.85±0.0001							

[a]Results are the mean of three independent experiments (n = 3) ± S.D.
[b]Selectivity for BChE = IC_{50} (AChE)/IC_{50} (BChE).

ligands, 4-Cl (**75**) has been found to be better inhibitor than 4-F (**78**) and 4-OH (**66**). On the other hand, electron withdrawing groups *e.g.,* NO_2 group especially at *ortho* and *para* positions was found to reduce the AChE inhibition. However, it is very hard to establish structure activity relationship of the studied escitalopram triazoles (**60-88**) probably due to the series of factors *i.e.,* size, shape, polarizability, and electronegativity of a ligand playing vital role in enzyme inhibition.

2.3.2. BChE Inhibition

BChE inhibition studies of triazoles **(60-88)** and tetrazole **(89)** of escitalopram are given in Table 2. The order of inhibition by the compounds is 2-F(**76**)>4-F(**78**)>4-OH-3-OCH_3(**88**)>2-I(**82**)>3-Cl(**74**)>3-F(**77**) with maximum inhibition by ligands **76** and **78** that have the lowest IC_{50}, 4.52±0.17 μM and 5.31±0.43 μM respectively. All these six compounds have been found highly active against BChE. The effect of substituents attached on the inhibition has been observed in the order of 2-F>4-F>4-OH-3-OCH_3>2-I>3-Cl>3-F.

It clearly demonstrates these groups once attached with the parent compound enhance the inhibitory activity of the enzyme. Compounds with IC_{50} values below 100 μM are in the order of 80>73>71>70 which correspond to 3-Br>2-Cl>3CH_3>2-CH_3. Other compounds showed high levels of IC_{50} values as given in Table 2. These compounds inhibited BChE with IC_{50} = 100 to 491.73 μM, exhibiting selectivity from 0.044- to < 49.08-fold more towards BChE than AChE.

Two members of this series have indicated poor AChE and BChE inhibition as compared to the standard eserine with the order 2-NO_2>4-Br. The compound **85** has not shown any activity against BChE.

The structure activity relationship has depicted the same but comparatively better trend of BChE inhibition than AChE inhibition. At *ortho*, *meta* and *para* positions mild electron donating groups enhance the BChE inhibition while electron withdrawing groups reduce the inhibition *e.g.,* NO_2 substituent especially at *ortho* position. However, the size and position of the substituents are important factors for the extent of the inhibition. In case of *ortho* substituted ligands, 2-F (**76**) has been found more active than others. The observed inhibition trend of *ortho* substituted ligands is as follow 2-F>2-I>2-Cl>2-CH_3>2-OH>2-NH_2>2-Br. In *meta* substituted 3-Cl (**74**) has been found more active than other with decreasing trend of 3-Cl>3-F>tetrazole>3-

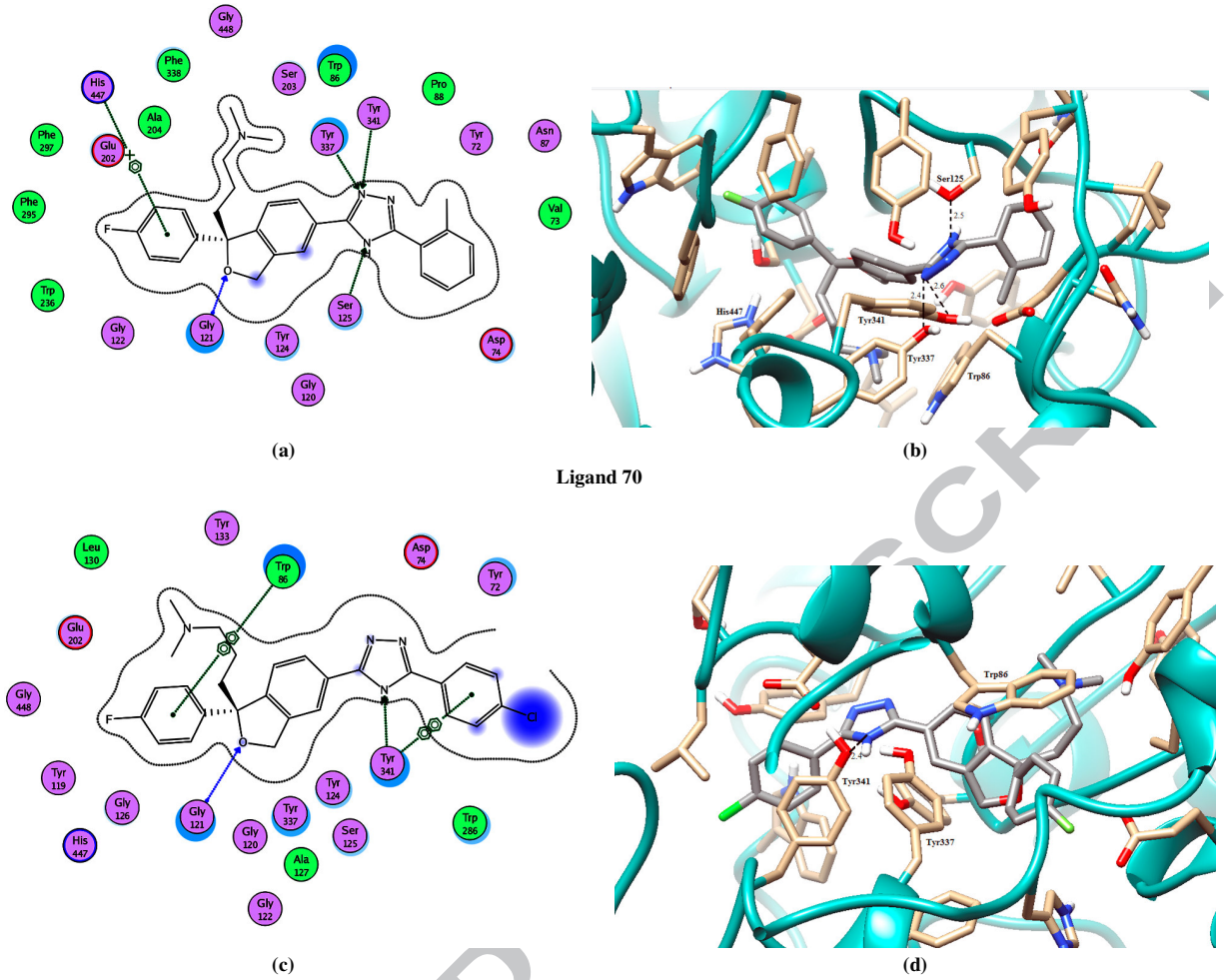

Figure 1. (a) and (c) represent 2D while (b) and (d) represent 3D view of the docked ligands **70** and **75** within AChE pocket. Dotted lines show the hydrogen bond interactions.

Br>3-CH_3>3-OCH_3>3-OH>3-NH_2 = 3-I. Tetrazole moiety (**89**) has showed moderate inhibition against BChE IC_{50} = 75.89 μM, exhibiting 3.32-fold more selective towards BChE than AChE.

The effect of para substituents on BChE inhibition have been found in the order of 4-F>4-OH-3-OCH_3>4-NH_2>4-OH>4-Cl>4-CH_3>4-I>4-OCH_3>4-Br. Again it is hard to make structure activity relationship of the escitalopram triazoles **(60-88)** against BChE because of the multiple factors involved between ligand and enzyme interaction. The different behavior of the ligands toward AChE and BChE is probably due to Van der Waal's weaker interactions between BChE and the ligands than those between AChE and the ligands perhaps because of a larger active site gorge and less important peripheral anionic site for BChE[27, 28] when compared to AChE[29]. It is also evident from the results that these compounds have selectivity; the compounds that have been active against AChE were not significantly active against BChE and vice versa.

Herein, the results clearly indicate that the novel escitalopram triazoles and tetrazole have shown good inhibitory activity against ChE, especially BChE, and can be used as an important starting point for further investigation of the possible use of these ligands in the drug discovery against neurodegenerative diseases.

2.3.4. Molecular Docking Studies

The X-ray crystallographic structures of AChE and BChE proteins were retrieved from RCSB Protein Data Bank (PDB ID 4m0e and PDB ID 4bds) respectively. The preparation of protein structure was done by removal of water molecules, co-factor and co-crystallized ligands by utilizing Discovery Studio 3.5 Visualizer. Molecular Operating Environment (MOE) program was used for ligand-receptor docking and binding energy calculations. Ligands **60-89** were docked with AChE (4m0e) and BChE (4bds) by MOE. The 3D coordinates files generation and energy minimization for each designed ligand was performed by using MOE builder. The addition of hydrogen atoms and energy minimization of receptor proteins was performed by using MOE. The default parameters of MOE-Dock program were selected to run the MOE Dock. Site Finder tool was utilized to select the binding pockets of AChE and BChE.

MOE *Site Finder* tool estimated 31 binding sites for AChE and 38 binding sites for BChE. The "site 1" was selected as binding pocket for docking analyses as it is surrounded by most critical residues indicated in crystal structure of AChE receptor (4m0e)[30, 31]. The docked structures were analyzed by using Ligand Interaction tool of MOE package.

The ligands were allowed to be flexible to obtain the correct conformations of the ligands. After the generation of docked complexes, the best conformations against AChE and BChE were analyzed for their binding interactions by using the ligand interaction tool of MOE. The binding affinities of the docked ligands were calculated as S-score (free binding energy or in ΔG_{bind} kcal/mol). Hydrogen bonding and hydrophobic interactions of each ligand were evaluated within binding pocket

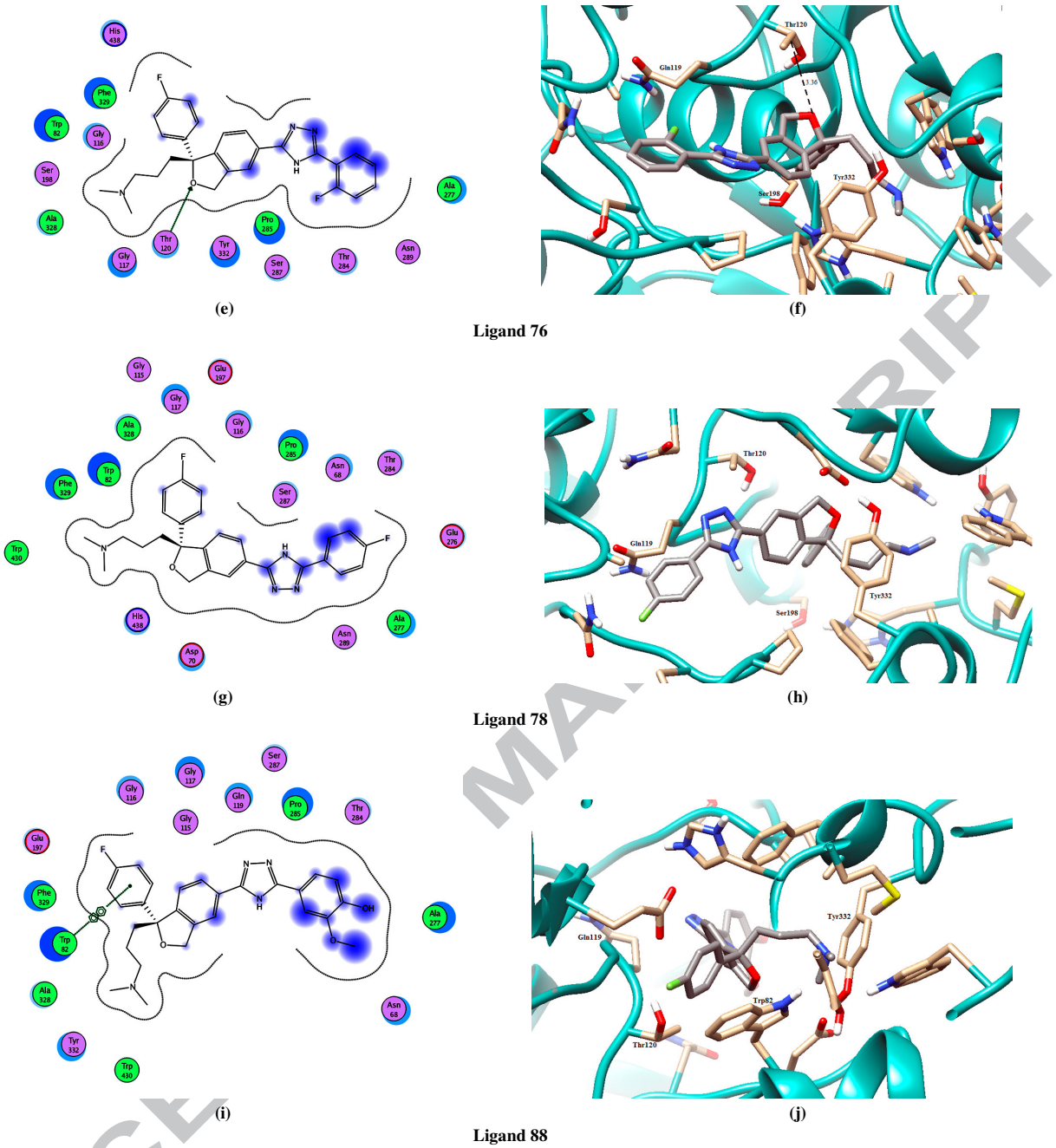

Figure 2. (e), (g) and (i) represent 2D while (f), (h) and (j) represent 3D view of the docked ligand **76, 78** and **88** within BChE pocket. Dotted lines show the hydrogen bond interactions.

of receptor protein. The conformation of the ligands which depicted the highest biological activities are exhibited in Figure 1 and Figure 2 along with their favorable interactions in the binding pockets of enzymes, while rest of the complexes and their interaction modes are available in the supporting information (Figures S1 and S2). The docked complexes of ligands **60-89** were analyzed to get qualitative assessment and to understand molecular basis of the calculated biological activities (IC_{50}) are showed in Table 3 and Table 4.

In case of AChE, the ligands **70** and **75** with highest IC_{50} values (Figure 1, Table 3) showed the binding affinities ΔG_{bind} (-6.42 and -6.93 kcal/mol) respectively. Visual inspection of these complexes predict such a binding conformation in which nitrogen of triazole ring of ligand **75** depicts potential for hydrogen bond with Tyr^{341} with an average distance of 2.4 Å and can play an important role to give comparatively superior binding affinity. The isobenzofuran scaffold shows a backbone hydrogen bond between its oxygen and Gly^{121} at an average distance of 3.1 Å. On the other hand, the terminal 4-chlorophenyl- ring attached with the triazole moiety was found to lie within a hydrophobic contact distance (3.2 Å) to Trp^{286}. Moreover, the terminal 4-chlorophenyl- and 4-fluorophenyl- rings form arene-arene contact potential with Tyr^{341} and Trp^{86} respectively. Investigation of the contacts between ligand **70** and AChE pocket reveals that NH of triazole ring form hydrogen bond with Ser^{125} (2.5 Å) and other nitrogen of triazole adjacent to the isobenzofuran scaffold form hydrogen bonds with Tyr^{341} and Tyr^{337} with an average distance of 2.4 and 2.6 Å respectively. Similarly, oxygen of

Table 3. Docking results for the highest ranked biologically active ligands (AChE).

Compd. No.[a]	ΔG_{bind}[b] (kcal/mol)	IC_{50}[c] (μM)	Amino acids show potential for		
			hydrogen bond contacts	arene-arene contacts	arene-cation contacts
60	-3.89	> 500	Tyr^{341}	Trp^{86}, Tyr^{341}	-
61	-4.02	359.72±0.34	Tyr^{72}, Gly^{121}	-	His^{447}
62	-4.03	> 500	Tyr^{341}	-	-
63	-3.38	-	Tyr^{341}	Tyr^{341}	-
64	-4.29	-	Tyr^{341}, Tyr^{124}, Tyr^{337}, Gly^{121}	Trp^{86}	His^{447}
65	-2.85	< 500	Ser^{203}, Tyr^{341}, Tyr^{72}	Trp^{86}, Tyr^{341}	-
66	-2.76	387.56±0.23	Gly^{121}, Tyr^{341}, Tyr^{124}, Trp^{86}, Gln^{71}	-	His^{447}
67	-2.72	-	Ser^{125}, Tyr^{341}	-	-
68	-6.15	138.23±0.17	Tyr^{341}	Tyr^{341}	-
69	-4.50	-	Gly^{121}, Tyr^{341}	Tyr^{341}	-
70	-6.42	9.52±0.23	Gly^{121}, Ser^{125}, Tyr^{341}, Tyr^{337}	-	His^{447}
71	-5.56	133.23±0.24	Trp^{86}, Tyr^{124}, Gly^{121}	-	-
72	-3.92	-	Tyr^{341}	Tyr^{341}	-
73	-3.68	-	Tyr^{133}, Ser^{125}	-	-
74	-1.66	412.56±0.45	Tyr^{337}	-	Tyr^{286}, Tyr^{341}
75	-6.93	6.71±0.25	Gly^{121}, Tyr^{341}	Tyr^{341}, Trp^{86}	-
76	-2.90	187.51±0.16	Trp^{86}, Gly^{121}, Tyr^{124}	-	His^{447}
77	-1.96	< 500	Tyr^{133}, Tyr^{341}	Tyr^{341}	-
78	-5.06	260.63±0.29	Ser^{203}	-	-
79	-2.71	-	Gly^{121}, Ser^{125}	-	His^{447}
80	-3.96	< 500	Gly^{121}, Tyr^{133}, Tyr^{341}	Tyr^{341}	-
81	-4.67	-	Asp^{74}, Gly^{121}, Tyr^{133}	Tyr^{341}	-
82	-1.24	310.31±0.28	Gly^{121}, Ser^{125}, Tyr^{337}	-	His^{447}
83	-4.81	> 500	Gly^{121}, Tyr^{337}	-	His^{447}
84	-2.98	> 500	Gly^{121}, Tyr^{341}	Trp^{86}, Tyr^{341}	-
85	-5.00	161.34±0.19	Gly^{121}, Ser^{125}, Ser^{125}	Trp^{86}	-
86	-2.94	123.77±0.32	Gly^{121}, Tyr^{341}	Trp^{86}, Tyr^{341}	-
87	-2.32	-	Ser^{125}, Tyr^{341}	Tyr^{341}	-
88	-2.82	< 500	Tyr^{124}, Ser^{125}, Gly^{121}	-	His^{447}
89	-5.56	251.67±0.14	Tyr^{337}	-	-

[a]No. = Specific code assigned to ligands.
[b]ΔG_{bind} = estimated Molecular Mechanics Generalized-Born Volume Integral (MM/GBVI)[32] binding free energy (Kcal/mol) calculated as "S score" by MOE docking software.
[c]IC_{50} = experimental calculation of inhibitory constant (μM).

isobenzofuran moiety accepts a hydrogen bond from Gly^{121} (2.3 Å). Whereas 4-fluorophenyl- ring forms arene-cation contact potential with His^{447}. Both the benzo moieties of the isobenzofuran and terminal 4-fluorophenyl-, and triazole ring were within potential for Van der waals contact distances from the hydrophobic side chains of the pocket amino acids Phe^{338} and Trp^{86}. Whereas other ligands of the series were found unable to show such a high binding energy profile.

On the other hand, binding energy calculations against BChE exhibited good trend as compared to AChE (Table 4). The binding affinities were observed for ligands **74, 76, 77, 78, 82** and **88** as shown by their ΔG_{bind} (-8.22, -9.04, -7.92, -8.51, -8.48 and -8.90 kcal/mol) respectively. The structural inspections of these complexes have shown that ligands **77, 78, 82** and **88** were unable to depict potential for hydrogen bonding. However, in case of ligand **76,** it can be observed that oxygen of isobenzofuran scaffold accepts a hydrogen bond from Thr^{120} with an average distance of 3.36 Å and hydrophobic contact potential with pocket amino acids Ala^{277}, Ala^{328}, Phe^{329}, Pro^{285}, Trp^{82} (Figure 2). Similarly, ligand **74** can form hydrogen bond between NH of triazole and Pro^{285} with an average distance of 1.91 Å. Moreover, ligands **74, 77, 78, 82** and **88** have shown the hydrophobic contacts potential with amino acid residues Trp^{82}, Ala^{328}, Phe^{329}; Trp^{231}, Pro^{285}, Phe^{329}, Ala^{328}, Trp^{82}, Ile^{69}; Pro^{285} Trp^{82}, Phe^{329} Ala^{328}, Ala^{277}; Trp^{82}, Phe^{329}, Pro^{285}, Ala^{328} and Pro^{285}, Ala^{277}, Phe^{329}, Ala^{328} respectively. The ligand **88** has depicted the arene-arene contact potential between 4-fluorophenyl- attached with the isobenzofuran and Trp^{82} amino acid (Figure 2). It's worth noting that hydrogen bonding and extensive hydrophobic interactions include arene-arene contact play a key role in giving ligands **76** and **88** superior inhibitory activities than other tested ligands. Moreover, the free rotation of the heterocyclic rings around the axis of the carbon linker permits the best orientation inside the binding pocket which is not permitted in other analogues.

3. Conclusion

Escitalopram triazoles **(60-88)** and tetrazole (**89**) have been designed, synthesized, characterized and analyzed against AChE and BChE. The results clearly show that escitalopram triazoles and tetrazole depict inhibitory activity against cholinesterases, especially BChE, and exhibit an interesting selectivity, being 0.044- to < 49.08-fold more active toward BChE than AChE. Two triazole derivatives of escitalopram 2-methyl- **(70)** and 4-

Table 4. Docking results for the highest ranked biologically active ligands (BChE).

Compd. No.[a]	ΔG_{bind}[b] (kcal/mol)	IC_{50}[c] (μM)	Amino acids show hydrogen bond contacts potential	Distance[d] (Å)	Amino acids show arene-arene contacts potential
60	-6.82	128.74±0.19	-	-	-
61	-7.04	110.53±0.11	Pro^{285}	1.86	-
62	-6.47	187.54±0.11	-	-	Tyr^{332}
63	-7.07	119.21±0.34	-	-	Trp^{82}
64	-7.72	101.52±0.27	Pro^{285}	2.06	-
65	-7.09	118.54±0.31	-	-	Trp^{82}
66	-7.19	140.22±0.29	Ser^{287}	1.44	-
67	-6.81	296.53±0.25	Pro^{285}	2.18	-
68	-7.86	105.23±0.18	-	-	Trp^{82}
69	-8.41	106.41±0.36	-	-	Trp^{82}
70	-6.79	99.74±0.32	-	-	Tyr^{332}
71	-7.81	89.24±0.28	-	-	-
72	-7.13	151.87±0.34	Pro^{285}	1.92	-
73	-6.92	81.41±0.21	-	-	-
74	-8.22	26.53±0.58	Pro^{285}	1.91	-
75	-6.98	151.35±0.23	-	-	-
76	-9.04	4.52±0.17	Thr^{120}	3.36	-
77	-7.92	44.83±0.35	-	-	-
78	-8.51	5.31±0.43	-	-	-
79	-7.45	140.93±0.16	-	-	-
80	-7.28	78.02±0.39	Pro^{285}	1.91	-
81	-6.90	491.73±0.32	Pro^{285}	2.04	-
82	-8.48	25.91±0.27	-	-	Tyr^{332}
83	-6.69	187.54±0.18	Pro^{285}	1.91	-
84	-6.25	160.95±0.33	-	-	Tyr^{332}
85	-7.18	-	-	-	Trp^{82}
86	-7.05	103.43±0.12	Asn^{289}	2.80	Tyr^{332}
87	-6.99	167.82±0.37	Asn^{289}	3.17	Tyr^{332}
88	-8.90	24.10±0.39	-	-	Trp^{82}
89	-6.46	75.89±0.14	Tyr^{128}	3.01	Trp^{82}

[a]No. = Specific code assigned to ligands.
[b]ΔG_{bind} = estimated Molecular Mechanics Generalized-Born Volume Integral (MM/GBVI)[32] binding free energy (Kcal/mol) calculated as "S score" by MOE docking software.
[c]IC_{50} = experimental calculation of inhibitory constant (μM).
[d]Distance = hydrogen bond length calculated from docked pose by using *Ligand interaction* tool of MOE.

chloro**- (75)** have depicted high AChE affinities, and five other analogues of this series *e.g.,* 3-NO_2- **(68),** 3-CH_3- **(71),** 2-F- **(76),** 2-OCH_3- **(85)** and 3-OCH_3- **(86)** have shown moderate AChE enzyme inhibition. It is clearly observed that electron donating groups at *ortho*, *meta* and *para* positions increase the inhibition while electron withdrawing substituents reduce the activity *e.g., o-* and *p*-NO_2 groups. The same trend of inhibition has been observed in BChE, in which *ortho*, *meta* and *para* substituted electron donating groups enhance the inhibition, while electron withdrawing groups reduce the inhibition *e.g.,* 2-NO_2. 2-Fluorophenyl- (**76**) and 4-fluorophenyl- (**78**) compounds were found to be excellent inhibitor of BChE. Four other compounds of the series have shown high BChE inhibition (IC_{50} < 82 μM) with the order: 4-OH-3-OCH_3>2-I>3-Cl>3F. Hence, 2-fluorophenyl- (**76**) and 4-fluorophenyl- (**78**) could be lead compounds of the series of escitalopram triazoles in case of BChE enzyme inhibition, and 2-methylphenyl- **(70)** and 4-chlorophenyl**- (75)** could be lead compounds in case AChE enzyme inhibition. These ligands can be modified by amending their structures to obtain therapeutically active agents against these enzymes and for the neurodegenerative diseases. The docking study revealed that in the binding pocket of AChE, ligands **70** and **75** have shown good binding affinities as depicted by their ΔG_{bind} -6.42 and -6.93 kcal/mol respectively, while in case of BChE, the ligands **74, 76, 77, 78, 82** and **88** are found to exhibit ΔG_{bind} -8.22, -9.04, -7.92, -8.51, -8.48 and -8.90 kcal/mol respectively.

4. Material and Methods

All chemicals were purchased from Sigma Aldrich Co. and Alfa Aesar and were used as received. ^{1}H NMR and ^{13}C spectra were recorded on a Bruker Advance-300 and 400 spectrometer. All NMR chemical shifts are reported as ppm relative to tetramethylsilane (TMS: δ = 0.00). Coupling constants (J) are reported in hertz. Spectra were processed with MestreNova and MestreC softwares. Mass spectra were taken in the positive ion mode under ESI methods. High resolution mass spectra were obtained on the 9.4 T Bruker FT-ICR-MS spectrometer in MeOH: MeCN (1: 1). The purity of compounds was determined by HPLC that was > 98% and completed on a Hewlett Packard 1100 [C-18, Microsorb-MV^{TM}, 4.6 mm x 250 mm, 5 µm]. 10-90% of methanol and acetonitrile with 0.1 % TFA within 30 min and up to 100% within extra 5 min, 1 mL/min, and TLC was determined on silica gel plates (Analtech 02521), solvent system EtOAc: hexanes (7: 3) and $CHCl_3$: CH_3OH (1: 1).

4.1. Synthesis of Benzohydrazides

4.1.1. *General procedure:*

Hydrazides (**30-58**) were synthesized by one pot conventional method[24] Benzoic acid or its derivative (10 mmol) was dissolved in ethanol (20 mL). Sulphuric acid (3N, 2 mL) was added and the reaction contents were refluxed for six hours. The reaction was

monitored with TLC. After the completion of the reaction, the reaction mixture was neutralized by adding solid $NaHCO_3$, and filtered to remove excess of $NaHCO_3$. In the neutralized reaction mixture which contains ethyl ester, hydrazine monohydrate (1.5 mL, 3 mmol) was added and refluxed for 3-6 hours to complete the reaction. Ethanol and unreacted hydrazine were removed by distillation upto 1/3 volume. The reaction contents were cooled, filtered and recrystallized from methanol to obtain the desired hydrazide crystals (See Supporting Information).

4.2. Synthesis of Escitalopram Triazoles

4.2.1. *General Procedure:*

The triazoles of escitalopram **(60-88)** were synthesized by following a reported method for triazole formation[25]. A mixture of a benzohydrazide (33 mmol), escitalopram (**59**-oxalate, 10 mmol) and K_2CO_3 (0.5 mmol) in n-butanol (2 mL) was heated at 150 ^oC for 5-6 hours. The reaction was monitored with TLC. After the completion of the reaction, the solvent was removed under reduced pressure. Finally, the triazole derivatives of escitalopram (**60-88**) were purified with column chromatography using solvent system CH_3OH/CH_3Cl = 60:40 and finally with preparative thin layer chromatography.

4.2.1.1. (*S*)-3-[1-(4-Fluorophenyl)-5-(5-phenyl-4*H*-1,2,4-triazol-3-yl)-1,3-dihydroisobenzofuran-1-yl]-*N,N*-dimethylpropan-1-amine (60) Brownish crystalline solid; Yield 4.0 g (90%); mp 188-189 ^oC; ^1H NMR (300 MHz, DMSO-d_6) δ_H: 8.43 (br s, 1NH), 7.99-7.78 (m, 5H), 7.67-7.48 (m, 3H), 7.24-7.03 (m, 3H), 5.21-5.10 (m, 2H), 2.42-2.36 (m, 2H), 2.20 (s, 6H), 1.40-1.17 (m, 4H); MS-(ESI) *m/z*: $[M+H]^+$, 443; HRMS: Calcd. for $C_{27}H_{28}FN_4O$: 443.2239; found: 443.2221. HPLC analysis: retention time = 13.1 min; peak area, 99.01%.

4.2.1.2. (*S*)-2-(5-{1-[3-(Dimethylamino)propyl]-1-(4-fluorophenyl)-1,3-dihydroisobenzofuran-5-yl}-4*H*-1,2,4-triazol-3-yl)aniline (61) Brownish yellow crystalline solid; Yield: 4.2 g (92%); mp 52-55 ^oC; ^1H NMR (300 MHz, DMSO-d_6) δ_H: 8.09 (br s, 1NH), 7.76-7.70 (m, 4H), 7.58-7.54 (m, 3H), 7.27-7.11 (m, 3H), 6.95-6.63 (m, 1H), 5.19-5.09 (m, 2H), 3.58 (s, 2H), 3.17-3.12 (m, 2H), 2.49 (s, 6H), 2.15-2.11 (m, 2H), 1.35-1.12 (m, 2H); MS-(ESI) *m/z*: $[M+H]^+$, 458; HRMS: Calcd. for $C_{27}H_{29}FN_5O$: 458.2343; found: 458.2333; . HPLC analysis: retention time = 12.2 min; peak area, 99.21%.

4.2.1.3. (*S*)-3-(5-{1-[3-(Dimethylamino)propyl]-1-(4-fluorophenyl)-1,3-dihydroisobenzofuran-5-yl}-4*H*-1,2,4-triazol-3-yl)aniline (62) Brownish yellow crystalline solid; Yield: 4.0 g (87%); mp 77-79 ^oC; ^1H NMR (300 MHz, DMSO-d_6) δ_H: 8.07 (br s, 1NH), 7.77-7.72 (m, 5H), 7.58-7.55 (m, 3H), 7.16-7.11 (m, 3H), 5.19-5.10 (m, 2H), 3.38 (s, 2H), 2.15-2.11 (m, 2H), 2.00 (s, 6H), 1.27-1.22 (m, 2H), 1.19-1.13 (m, 2H); MS-(ESI) *m/z*: $[M+H]^+$, 458; HRMS: Calcd. for $C_{27}H_{29}FN_5O$: 458.2341; found: 458.2359; HPLC analysis: retention time = 12.9 min; peak area, 99.45%.

4.2.1.4. (*S*)-4-(5-{1-(3-[Dimethylamino)propyl]-1-(4-fluorophenyl)-1,3-dihydroisobenzofuran-5-yl}-4*H*-1,2,4-triazol-3-yl)aniline (63) Brownish yellow crystalline solid; Yield: 4.35 g (95%); mp 95-98 ^oC; ^1H NMR (300 MHz, DMSO-d_6) δ_H: 8.52 (br s, 1NH), 7.85-7.78 (m, 5H), 7.65-7.57 (m, 3H), 7.28-7.14 (m, 3H), 5.23-5.15 (m, 2H), 3.53 (s, 2H), 3.26-3.13 (m, 2H), 2.97 (s, 6H), 2.17-2.11 (m, 2H), 1.26-1.21 (m, 2H); MS-(ESI) *m/z*: $[M+H]^+$, 458; HRMS: Calcd. for $C_{15}H_{27}N_4O_7$: 458.2345; found: 458.2357; . HPLC analysis: retention time = 12.8 min; peak area, 99.77%.

4.2.1.5. (*S*)-2-(5-{1-[3-(Dimethylamino)propyl]-1-(4-fluorophenyl)-1,3-dihydroisobenzofuran-5-yl}-4*H*-1,2,4-triazol-3-yl)phenol (64) Brownish crystalline solid; Yield: 4.27 g (93%); mp 135-137 ^oC; ^1H NMR (300 MHz, DMSO-d_6) δ_H: 8.14 (br s, 1NH), 7.78-7.71 (m, 5H), 7.57-7.54 (m, 3H), 7.15 (t, J = 8.7 Hz, 3H), 5.21-5.10 (m, 2H), 3.91 (s, 1H), 3.55-3.33 (m, 2H), 2.78 (s, 6H), 2.21-2.17 (m, 2H), 1.52-1.44 (m, 2H); MS-(ESI) *m/z*: $[M+H]^+$, 459; HRMS: Calcd. for $C_{27}H_{28}FN_4O_2$: 459.2191; found: 459.2199; . HPLC analysis: retention time = 13.3 min; peak area, 98.11%.

4.2.1.6. (*S*)-3-(5-{1-[3-(Dimethylamino)propyl]-1-(4-fluorophenyl)-1,3-dihydroisobenzofuran-5-yl}-4*H*-1,2,4-triazol-3-yl)phenol (65) Brownish crystalline solid; Yield 4.16 g (91%); mp 140-143 ^oC; ^1H NMR (300 MHz, DMSO-d_6) δ_H: 8.07 (br s, 1NH), 7.80-7.73 (m, 5H), 7.59-7.56 (m, 3H), 7.18 (t, J = 8.2 Hz, 3H), 5.23-5.12 (m, 2H), 3.94 (s, 1H), 3.39-3.31 (m, 2H), 2.72 (s, 6H), 2.21-2.18 (m, 2H), 1.55-1.47 (m, 2H); ^{13}C NMR (100 MHz, CD_3OD) δ_C: 160.84, 157.99, 157.47, 149.44, 141.20, 140.32, 135.45, 131.88, 130.84, 129.26, 129.21, 129.15, 128.32, 125.22, 122.80, 118.64, 115.46, 111.76, 91.12, 71.26, 62.97, 45.16, 38.90, 21.96; MS-(ESI) *m/z*: $[M+H]^+$: 459; HRMS: Calcd. for $C_{27}H_{28}FN_4O_2$: 459.2193; found: 459.2189; . HPLC analysis: retention time = 13.6 min; peak area, 99.05%.

4.2.1.7. (*S*)-4-(5-{1-[3-(Dimethylamino)propyl]-1-(4-fluorophenyl)-1,3-dihydroisobenzofuran-5-yl}-4*H*-1,2,4-triazol-3-yl)phenol (66) Brownish crystalline solid; Yield: 4.37 g (95%); mp 165-167 ^oC; ^1H NMR (300 MHz, DMSO-d_6) δ_H: 9.44 (br s, 1NH), 7.66-7.62 (m, 4H), 6.79-6.73 (m, 7H), 5.17-5.08 (m, 2H), 4.11 (s, 1H), 3.14-3.10 (m, 2H), 1.99 (s, 6H), 2.14-2.10 (m, 2H), 1.14-1.12 (m, 2H); MS-(ESI) *m/z*: $[M+H]^+$, 459; HRMS: Calcd. for $C_{27}H_{28}FN_4O_2$: 459.2190; found: 459.2198; . HPLC analysis: retention time = 13.4 min; peak area, 99.13%.

4.2.1.8. (*S*)-3-{1-(4-Fluorophenyl)-5-[5-(2-nitrophenyl)-4*H*-1,2,4-triazol-3-yl]-1,3-dihydroisobenzofuran-1-yl}-*N,N*-dimethylpropan-1-amine (67) Yellowish brown crystalline solid; Yield: 4.39 g (90%); mp 191-194 ^oC; ^1H NMR (300 MHz, DMSO-d_6) δ_H: 8.02 (br s, 1NH), 7.79-7.70 (m, 5H), 7.60-7.54 (m, 3H), 7.17-7.12 (m, 3H), 5.23-5.12 (m, 2H), 3.16 (t, J = 6.3 Hz, 2H), 2.93 (s, 6H), 2.20-2.15 (m, 2H), 1.61-1.52 (m, 2H); MS-(ESI) *m/z*: $[M+H]^+$, 488; HRMS: Calcd. for $C_{27}H_{27}FN_5O_3$: 488.2095; found: 488.2090; . HPLC analysis: retention time = 14.2 min; peak area, 99.31%.

4.2.1.9. (*S*)-3-{1-(4-Fluorophenyl)-5-[5-(3-nitrophenyl)-4*H*-1,2,4-triazol-3-yl]-1,3-dihydroisobenzofuran-1-yl}-*N,N*-dimethylpropan-1-amine (68) Yellowish brown crystalline solid; Yield: 4.19 g (86%); mp 205-207 ^oC; ^1H NMR (300 MHz, DMSO-d_6) δ_H: 8.44 (br s, 1NH), 7.90-7.78 (m, 5H), 7.61-7.42 (m, 3H), 7.26-7.06 (m, 3H), 5.30-5.11 (m, 2H), 3.40-3.23 (m, 2H), 2.48 (s, 6H), 2.25-2.18 (m, 2H), 1.28-1.14 (m, 2H); MS-(ESI) *m/z*: $[M+H]^+$, 488; HRMS: Calcd. for $C_{27}H_{27}FN_5O_3$: 488.2091; found: 488.2100; . HPLC analysis: retention time = 14.0 min; peak area, 99.19%.

4.2.1.10. (*S*)-3-{1-(4-Fluorophenyl)-5-[5-(4-nitrophenyl)-4*H*-1,2,4-triazol-3-yl]-1,3-dihydroisobenzofuran-1-yl}-*N,N*-dimethylpropan-1-amine (69) Yellowish brown crystalline solid; Yield: 4.44 g (91%); mp 221-223 ^oC; ^1H NMR (300 MHz, DMSO-d_6) δ_H: 8.32 (br s, 1NH), 7.79-7.62 (m, 5H), 7.57-7.55 (m, 3H), 7.18 (t, J = 8.7 Hz, 3H), 5.23-5.11 (m, 2H), 2.78-2.75 (m,

2H), 2.20 (s, 6H), 1.50-1.33 (m, 2H), 1.28-1.21 (m, 2H); MS-(ESI) *m/z*: $[M+H]^+$, 488; HRMS: Calcd. for $C_{27}H_{27}FN_5O_3$: 488.2094; found: 488.2088; . HPLC analysis: retention time = 14.4 min; peak area, 99.38%.

4.2.1.11. (*S*)-3-{1-(4-Fluorophenyl)-5-[5-(o-tolyl)-4*H*-1,2,4-triazol-3-yl]-1,3-dihydroisobenzofuran-1-yl}-*N,N*-dimethylpropan-1-amine (70) Brown crystalline solid; Yield: 4.12 g (90%); mp 109-111 °C; ^{1}H NMR (300 MHz, DMSO-d_6) δ_H: 8.41 (br s, 1NH), 7.77-7.55 (m, 7H), 7.26-7.14 (m, 4H), 5.33-5.02 (m, 2H), 3.30-3.21 (m, 2H), 2.66-2.63 (m, 2H), 2.47 (s, 6H), 2.30 (s, 3H), 1.39-1.20 (m, 2H); MS-(ESI) *m/z*: $[M+H]^+$, 457; HRMS: Calcd. for $C_{28}H_{30}FN_4O$: 457.2400; found: 457.2408; . HPLC analysis: retention time = 15.1 min; peak area, 99.15%.

4.2.1.12. (*S*)-3-{1-(4-Fluorophenyl)-5-[5-(m-tolyl)-4*H*-1,2,4-triazol-3-yl]-1,3-dihydroisobenzofuran-1-yl}-*N,N*-dimethylpropan-1-amine (71) Brown crystalline solid; Yield: 4.26 g (93%); mp 125-127 °C; ^{1}H NMR (300 MHz, DMSO-d_6) δ_H: 8.13 (br s, 1NH), 7.79-7.71 (m, 5H), 7.58-7.54 (m, 3H), 7.17-7.11 (m, 3H), 5.20-5.10 (m, 2H), 2.82 (t, *J* = 5.7 Hz, 2H), 2.61 (s, 6H), 2.43-2.42 (m, 2H), 2.35 (s, 3H), 2.24-2.13 (m, 2H); MS-(ESI) *m/z*: $[M+H]^+$, 457; HRMS: Calcd. for $C_{28}H_{30}FN_4O$: 457.2402; found: 457.2411; . HPLC analysis: retention time = 15.3 min; peak area, 99.03%.

4.2.1.13. (*S*)-3-{1-(4-Fluorophenyl)-5-[5-(p-tolyl)-4*H*-1,2,4-triazol-3-yl]-1,3-dihydroisobenzofuran-1-yl}-*N,N*-dimethylpropan-1-amine (72) Brown crystalline solid; Yield: 4.37 g (96%); mp 78-80 °C; ^{1}H NMR (300 MHz, DMSO-d_6) δ_H: 7.93 (br s, 1NH), 7.77-7.72 (m, 5H), 7.58-7.55 (m, 3H), 7.15-7.11 (m, 3H), 5.20-5.10 (m, 2H), 3.21-3.15 (m, 2H), 2.49 (s, 3H), 2.13-2.10 (m, 2H), 1.99 (s, 6H), 1.27-1.19 (m, 2H); MS-(ESI) *m/z*: $[M+H]^+$, 457; HRMS: Calcd. for $C_{28}H_{30}FN_4O$: 457.2407; found: 457.2415; HPLC analysis: retention time = 15.6 min; peak area, 99.53%.

4.2.1.14. (*S*)-3-{5-[5-(2-Chlorophenyl)-4*H*-1,2,4-triazol-3-yl]-1-(4-fluorophenyl)-1,3-dihydroisobenzofuran-1-yl}-*N,N*-dimethylpropan-1-amine (73) Colorless crystalline solid; Yield: 4.21 g (88%); mp 211-214 °C; ^{1}H NMR (300 MHz, DMSO-d_6) δ_H: 8.30 (s, 1H), 7.82-7.74 (m, 5H), 7.62-7.57 (m, 3H), 7.21 (t, *J* = 9.0 Hz, 3H), 5.25-5.14 (m, 2H), 2.45 (s, 6H), 2.23 (t, *J* = 7.2 Hz, 2H), 1.59-1.40 (m, 2H), 1.36-1.29 (m, 2H); MS-(ESI) *m/z*: $[M+H]^+$, 477, 479; HRMS: Calcd. for $C_{27}H_{27}ClFN_4O$: 477.1852; found: 477.1861; HPLC analysis: retention time = 12.0 min; peak area, 99.43%.

4.2.1.15. (*S*)-3-{5-[5-(3-Chlorophenyl)-4*H*-1,2,4-triazol-3-yl]-1-(4-fluorophenyl)-1,3-dihydroisobenzofuran-1-yl}-*N,N*-dimethylpropan-1-amine (74) Colorless crystalline solid; Yield: 4.11 g (86%); mp 233-236 °C; ^{1}H NMR (300 MHz, DMSO-d_6) δ_H: 8.11 (br s, 1NH), 7.73-7.69 (m, 5H), 7.57-7.52 (m, 3H), 7.14 (t, *J* = 8.7 Hz, 3H), 5.18-5.07 (m, 2H), 2.00 (s, 6H), 2.14-2.10 (m, 2H), 1.28-1.11 (m, 4H); MS-(ESI) *m/z*: $[M+H]^+$, 477, 479; HRMS: Calcd. for $C_{27}H_{27}ClFN_4O$: 477.1855; found: 477.1867; HPLC analysis: retention time = 12.3 min; peak area, 99.36%.

4.2.1.16. (*S*)-3-{5-[5-(4-Chlorophenyl)-4*H*-1,2,4-triazol-3-yl]-1-(4-fluorophenyl)-1,3-dihydroisobenzofuran-1-yl}-*N,N*-dimethylpropan-1-amine (75) Colorless crystalline solid; Yield: 4.31 g (91%); mp 280-282 °C; ^{1}H NMR (300 MHz, DMSO-d_6) δ_H: 8.09 (br s, 1NH), 7.81-7.74 (m, 5H), 7.61-7.57 (m, 3H), 7.18 (t, *J* = 8.7 Hz, 3H), 5.24-5.13 (m, 2H), 2.90-2.86 (m, 2H), 2.54 (s, 6H), 2.26-2.22 (m, 2H), 1.54-1.38 (m, 2H); MS-(ESI) *m/z*: $[M+H]^+$, 477, 479; HRMS: Calcd. for $C_{27}H_{27}ClFN_4O$: 477.1855; found: 477.1860; HPLC analysis: retention time = 12.5 min; peak area, 99.47%.

4.2.1.17. (*S*)-3-{1-(4-Fluorophenyl)-5-[5-(2-fluorophenyl)-4*H*-1,2,4-triazol-3-yl]-1,3-dihydroisobenzofuran-1-yl}-*N,N*-dimethylpropan-1-amine (76) Colorless crystalline solid; Yield: 4.29 g (93%); mp 153-156 °C; ^{1}H NMR (300 MHz, DMSO-d_6) δ_H: 7.87 (br s, 1NH), 7.78-7.73 (m, 5H), 7.60-7.56 (m, 3H), 7.17-7.12 (m, 3H), 5.21-5.11 (m, 2H), 2.17-2.14 (m, 4H), 2.02 (s, 6H), 1.29-1.23 (m, 2H); MS-(ESI) *m/z*: $[M+H]^+$, 461; HRMS: Calcd. for $C_{27}H_{27}F_2N_4O$: 461.2150; found: 461.2157; HPLC analysis: retention time = 13.5 min; peak area, 99.67%.

4.2.1.18. (*S*)-3-{1-(4-Fluorophenyl)-5-[5-(3-fluorophenyl)-4*H*-1,2,4-triazol-3-yl]-1,3-dihydroisobenzofuran-1-yl}-*N,N*-dimethylpropan-1-amine (77) Colorless crystalline solid; Yield: 4.0 g (87%); mp 187-189 °C; ^{1}H NMR (300 MHz, DMSO-d_6) δ_H: 8.24 (br s, 1NH), 7.78-7.68 (m, 5H), 7.60-7.56 (m, 3H), 7.18 (t, *J* = 9.0 Hz, 3H), 5.22-5.10 (m, 2H), 2.19-2.13 (m, 2H), 2.04 (s, 6H), 1.37-1.24 (m, 2H), 1.22-1.14 (m, 2H); MS-(ESI) *m/z*: $[M+H]^+$, 461; HRMS: Calcd. for $C_{27}H_{27}F_2N_4O$: 461.2151; found: 461.2155; HPLC analysis: retention time = 13.4 min; peak area, 99.47%.

4.2.1.19. (*S*)-3-{1-(4-Fluorophenyl)-5-[5-(4-fluorophenyl)-4*H*-1,2,4-triazol-3-yl]-1,3-dihydroisobenzofuran-1-yl}-*N,N*-dimethylpropan-1-amine (78) Colorless crystalline solid; Yield: 4.38 g (95%); mp 163-165 °C; ^{1}H NMR (300 MHz, DMSO-d_6) δ_H: 8.06 (br s, 1NH), 7.77-7.71 (m, 5H), 7.59-7.54 (m, 3H), 7.16 (t, *J* = 8.7 Hz, 3H), 5.20-5.08 (m, 2H), 2.14 (t, *J* = 7.6 Hz, 2H), 1.99 (s, 6H), 1.76-1.74 (m, 2H), 1.27-1.13 (m, 2H); ^{13}C NMR (100 MHz, CD_3OD) δ_C: 163.24, 160.79, 153.15, 149.53, 140.32, 139.59, 131.85, 126.81, 126.73, 125.21, 122.79, 118.66, 115.41, 115.20, 111.68, 91.11, 71.30, 59.36, 45.26, 38.91, 22.07; MS-(ESI) *m/z*: $[M+H]^+$, 461; HRMS: Calcd. for $C_{27}H_{27}F_2N_4O$: 461.2150; found: 461.2161; HPLC analysis: retention time = 13.2 min; peak area, 99.33%.

4.2.1.20. (*S*)-3-{5-[5-(2-Bromophenyl)-4*H*-1,2,4-triazol-3-yl]-1-(4-fluorophenyl)-1,3-dihydroisobenzofuran-1-yl}-*N,N*-dimethylpropan-1-amine (79) Brownish crystalline solid; Yield: 4.23 g (81%); mp 141-143 °C; ^{1}H NMR (300 MHz, DMSO-d_6) δ_H: 7.87 (br s, 1NH), 7.78-7.71 (m, 5H), 7.58-7.54 (m, 3H), 7.16-7.10 (m, 3H), 5.20-5.09 (m, 2H), 2.20-2.15 (m, 2H), 2.03 (s, 6H), 1.45-1.33 (m, 2H), 1.27-1.17 (m, 2H); MS-(ESI) *m/z*: $[M+H]^+$, 521, 523; HRMS: Calcd. for $C_{27}H_{27}BrFN_4O$: 521.1349; found: 521.1357; HPLC analysis: retention time = 14.2 min; peak area, 99.21%.

4.2.1.21. (*S*)-3-{5-[5-(3-Bromophenyl)-4*H*-1,2,4-triazol-3-yl]-1-(4-fluorophenyl)-1,3-dihydroisobenzofuran-1-yl}-*N,N*-dimethylpropan-1-amine (80) Brownish crystalline solid; Yield: 4.13 g (79%); mp 121-123 °C; ^{1}H NMR (300 MHz, DMSO-d_6) δ_H: 7.76-7.73 (m, 5H), 7.71 (s, 1NH), 7.58-7.54 (m, 3H), 7.16 (t, *J* = 9.0 Hz, 3H), 5.20-5.08 (m, 2H), 2.14-2.09 (m, 2H), 1.99 (s, 6H), 1.34-1.23 (m, 2H), 1.21-1.19 (m, 2H); MS-(ESI) *m/z*: $[M+H]^+$, 521, 523; HRMS: Calcd. for $C_{27}H_{27}BrFN_4O$: 521.1351; found: 521.1355; HPLC analysis: retention time = 14.5 min; peak area, 99.38%.

4.2.1.22. (*S*)-3-{5-[5-(4-Bromophenyl)-4*H*-1,2,4-triazol-3-yl]-1-(4-fluorophenyl)-1,3-dihydroisobenzofuran-1-yl}-*N,N*-dimethylpropan-1-amine (81) Brownish crystalline solid; mp 158-161 °C; Yield: 4.37 g (84%); ^{1}H NMR (300 MHz, DMSO-d_6) δ_H: 7.85 (br s, 1NH), 7.77-7.71 (m, 5H), 7.59-7.54 (m, 3H), 7.16 (t, *J* = 8.7 Hz, 3H), 5.20-5.09 (m, 2H), 2.18-2.14 (m, 2H), 2.04 (s, 6H), 1.33-1.23 (m, 2H), 1.20-1.11 (m, 2H); MS-(ESI) *m/z*:

$[M+H]^+$, 521, 523; HRMS: Calcd. for $C_{27}H_{27}BrFN_4O$: 521.1348; found: 521.1359; HPLC analysis: retention time = 14.3 min; peak area, 99.55%.

4.2.1.23. (*S*)-3-{1-(4-Fluorophenyl)-5-[5-(2-iodophenyl)-4*H*-1,2,4-triazol-3-yl]-1,3-dihydroisobenzofuran-1-yl}-*N,N*-dimethylpropan-1-amine (82) Colorless crystalline solid; Yield: 4.0 g (70%); mp 101-104 °C; ^{1}H NMR (300 MHz, DMSO-d_6) δ_H: 8.08 (br s, 1NH), 7.77-7.72 (m, 5H), 7.58-7.54 (m, 3H), 7.15-7.11 (m, 3H), 5.19-5.09 (m, 2H), 2.14-2.10 (m, 2H), 1.99 (s, 6H), 1.34-1.22 (m, 2H), 1.21-1.15 (m, 2H); MS-(ESI) *m/z*: $[M+H]^+$, 569; HRMS: Calcd. for $C_{27}H_{27}FIN_4O$: 569.1210; found: 569.1217; HPLC analysis: retention time = 14.9 min; peak area, 99.78%.

4.2.1.24. (*S*)-3-{1-(4-Fluorophenyl)-5-[5-(3-iodophenyl)-4*H*-1,2,4-triazol-3-yl]-1,3-dihydroisobenzofuran-1-yl}-*N,N*-dimethylpropan-1-amine (83) Colorless crystalline solid; Yield: 4.08 g (72%); mp 117-120 °C; ^{1}H NMR (300 MHz, DMSO-d_6) δ_H: 8.10 (br s, 1NH), 7.77-7.72 (m, 4H), 7.58-7.55 (m, 3H), 7.16-7.11 (m, 4H), 5.20-5.10 (m, 2H), 2.28-2.24 (m, 2H), 2.18-2.13 (m, 2H), 2.10 (s, 6H), 1.26-1.21 (m, 2H); MS-(ESI) *m/z*: $[M+H]^+$, 569; HRMS: Calcd. for $C_{27}H_{27}FIN_4O$: 569.1212; found: 569.1220; HPLC analysis: retention time = 14.7 min; peak area, 99.67%.

4.2.1.25. (*S*)-3-{1-(4-Fluorophenyl)-5-[5-(4-iodophenyl)-4*H*-1,2,4-triazol-3-yl]-1,3-dihydroisobenzofuran-1-yl}-*N,N*-dimethylpropan-1-amine (84) Colorless crystalline solid; Yield: 4.27 g (75%); mp 137-140 °C; ^{1}H NMR (300 MHz, DMSO-d_6) δ_H: 8.13 (br s, 1NH), 7.75-7.70 (m, 5H), 7.57-7.54 (m, 3H), 7.14-7.09 (m, 3H), 5.18-5.09 (m, 2H), 2.49-2.47 (m, 2H), 2.11-2.08 (m, 2H), 1.97 (s, 6H), 1.26-1.17 (m, 2H); MS-(ESI) *m/z*: $[M+H]^+$, 569; HRMS: Calcd. for $C_{27}H_{27}FIN_4O$: 569.1209; found: 569.1214; HPLC analysis: retention time = 14.8 min; peak area, 99.87%.

4.2.1.26. (*S*)-3-{1-(4-Fluorophenyl)-5-[5-(2-methoxyphenyl)-4*H*-1,2,4-triazol-3-yl]-1,3-dihydroisobenzofuran-1-yl}-*N,N*-dimethylpropan-1-amine (85) Brownish yellow crystalline solid; Yield: 4.15 g (88%); mp 131-134 °C; ^{1}H NMR (300 MHz, DMSO-d_6) δ_H: 8.43 (br s, 1NH), 7.98-7.59 (m, 8H), 7.34-7.15 (m, 3H), 5.26-5.16 (m, 2H), 3.38 (s, 3H), 2.81-2.69 (m, 2H), 2.49 (s, 6H), 2.34-2.23 (m, 2H), 1.47-1.23 (m, 2H); MS-(ESI) *m/z*: $[M+H]^+$, 473; HRMS: Calcd. for $C_{28}H_{30}FN_4O_2$: 473.2347; found: 473.2355; HPLC analysis: retention time = 12.3 min; peak area, 98.91%.

4.2.1.27. (*S*)-3-{1-(4-Fluorophenyl)-5-[5-(3-methoxyphenyl)-4*H*-1,2,4-triazol-3-yl]-1,3-dihydroisobenzofuran-1-yl}-*N,N*-dimethylpropan-1-amine (86) Brownish yellow crystalline solid; Yield: 4.05 g (86%); mp 139-142 °C; ^{1}H NMR (300 MHz, DMSO-d_6) δ_H: 8.41 (br s, 1NH), 7.78-7.71 (m, 5H), 7.57-7.54 (m, 3H), 7.15-7.10 (m, 3H), 5.20-5.09 (m, 2H), 3.70 (s, 3H), 3.36-3.34 (m, 4H), 2.47 (s, 6H), 2.26-2.17 (m, 2H); MS-(ESI) *m/z*: $[M+H]^+$, 473; HRMS: Calcd. for $C_{28}H_{30}FN_4O_2$: 473.2349; found: 473.2358; HPLC analysis: retention time = 12.1 min; peak area, 99.11%.

4.2.1.28. (*S*)-3-{1-(4-Fluorophenyl)-5-[5-(4-methoxyphenyl)-4*H*-1,2,4-triazol-3-yl]-1,3-dihydroisobenzofuran-1-yl}-*N,N*-dimethylpropan-1-amine (87) Brownish yellow crystalline solid; Yield: 4.24 g (90%); mp 150-152 °C; ^{1}H NMR (300 MHz, DMSO-d_6) δ_H: 8.11 (br s, 1NH), 7.78-7.73 (m, 5H), 7.59-7.55 (m, 2H), 7.16-7.12 (m, 4H), 5.20-5.10 (m, 2H), 3.37 (s, 3H), 2.18-2.11 (m, 4H), 2.00 (s, 6H), 1.29-1.17 (m, 2H); MS-(ESI) *m/z*: $[M+H]^+$, 473; HRMS: Calcd. for $C_{28}H_{30}FN_4O_2$: 473.2352; found: 473.2363; HPLC analysis: retention time = 12.4 min; peak area, 99.41%.

4.2.1.29. (*S*)-4-(5-{1-[3-(Dimethylamino)propyl]-1-(4-fluorophenyl)-1,3-dihydroisobenzofuran-5-yl)-4*H*-1,2,4-triazol-3-yl}-2-methoxyphenol (88) Brown crystalline solid; Yield: 4.31 g (88%); mp 199-201 °C; ^{1}H NMR (300 MHz, DMSO-d_6) δ_H: 7.91 (br s, 1NH), 7.75-7.70 (m, 5H), 7.56-7.53 (m, 3H), 7.14-7.09 (m, 3H), 5.17-5.08 (m, 2H), 3.62 (s, 1H), 3.33 (s, 3H), 2.14-2.07 (m, 2H), 1.97 (s, 6H), 1.25-1.16 (m, 4H); MS-(ESI) *m/z*: $[M+H]^+$, 489; HRMS: Calcd. for $C_{28}H_{30}FN_4O_3$: 489.2298; found: 489.2309; HPLC analysis: retention time = 13.9 min; peak area, 99.58%.

4.3. Synthesis of Tetrazole of Escitalopram

4.3.1. (*S*)-3-[1-(4-Fluorophenyl)-5-(1*H*-tetrazol-5-yl)-1,3-dihydroisobenzofuran-1-yl]-*N,N*-dimethylpropan-1-amine (89) Tetrazole of escitalopram (**89**) was synthesized by following the method described in literature for tetrazole formation[26]. Escitalopram (**59**-oxalate, 4.14 g, 10 mmol), sodium azide (0.65 g, 10 mmol) and ammonium chloride (0.53 g, 10 mmol) were dissolved in DMF (10 mL) and heated on an oil bath for 7 hours at 125 °C. The reaction was monitored with TLC. After completion of the reaction, solvent was removed under reduced pressure. The residue was dissolved in 100 mL of water and carefully acidified with conc. HCl to pH 2. The dark brown thick oil was extracted with ethyl acetate. The solvent was evaporated and the residue was purified using column chromatography using solvent system CH_3OH: CH_3Cl (50:50) and further purified with RP-HPLC for analytical purpose. Colorless crystalline solid; Yield: 3.35 g (91%); mp 214-216 °C; retention time: 24.6; ^{1}H NMR (400 MHz, DMSO-d_6) δ_H: 7.56-7.43 (m, 2H), 7.07-6.69 (m, 5H), 6.01 (br s, 1NH), 4.58-4.50 (s, 2H), 2.25-2.10 (m, 2H), 2.01 (s, 6H), 1.75-1.66 (m, 2H), 1.16-1.06 (m, 2H); ^{13}C NMR (100 MHz, CD_3OD) δ_C: 160.31, 155.27, 140.42, 139.11, 135.91, 129.44, 129.38, 128.14, 128.09, 125.98, 114.74, 90.22, 71.18, 51.25, 44.12, 40.08, 18.37; MS-(ESI) *m/z*: $[M+H]^+$, 368; HRMS: Calcd. for $C_{20}H_{23}N_5O$: 368.1883; found: 368.1889; HPLC analysis: retention time = 11.1 min; peak area, 99.31%.

4.4. AChE and BChE Assay

The AChE and BChE inhibition activity was accomplished by the reported method[43] with slight alterations. The reaction mixture was consisted of 100 μL of the total volume. It contained Na_2HPO_4 buffer 60 μL with pH 7.7 and 50 mM concentration. To this solution the test compound (0.5 mM well^{-1} 10 μL) was added in the 96-well plate followed by the addition of 10 μL (0.01 unit well^{-1}, 0.005 units) enzyme. The reaction contents were thoroughly mixed, pre-incubated for 10 min at 37 ºC and pre-read at 405 nm. The reaction started by the addition of 10 μL of 0.5 mM well^{-1} substrate (acetylthiocholine iodide, butyrylthiocholine chloride), followed by the incorporation of 10 μL of 0.5 mM well^{-1} Ellman solution (DTNB). After 30 min of incubation at 37 ºC, absorbance was recorded at 405 nm by 96-well plate reader Synergy HT, Biotek, USA. All experiments were performed with their respective standards (controls) in triplicate. As a positive control Eserine (0.5 mM well^{-1}) was practiced. The percent inhibition was measured by following equation

$$\text{Inhibition (\%)} = (\text{Control} - \text{Test} / \text{Control}) \times 100$$

The IC_{50} values of active compounds were determined by assaying the serial dilutions and data was computed by EZ–Fit

Enzyme kinetics software (Perrella Scientific Inc. Amherst, USA).

Acknowledgments

We gratefully acknowledge a grant given from the Higher Education Commission of Pakistan under the Indigenous programme to support Mehr-un-Nisa.

Supplementary Material

^{1}H NMR, ^{13}C NMR and Mass spectra of the ligands **60-89** are provided.

References

1. Silman, I. and Sussman, J. L. Structural studies on cholinesterases. In: *cholinesterases and Cholinesterase Inhibitors.* Giacobini, E., Ed.; Mortin Dunitz: London, **2000**; pp. 9–25.
2. Nachmensohn, D. *Chemical and molecular basis of nerve activity.* Physiologically significant features of acetylcholinesterase & Academic Press: New York and London, **1959**.
3. Taylor, P. Anticholinesterase agents. In *The Pharmalogical Basis of Therapeutics.* Hardman, J. G.; Limbird, L. E.; Molinoff, P. B.; Ruddon, R. W. and Gilman, A. G., Eds.; McGraw-Hill: New York, **1996**; pp. 161–176.
4. Giacobini, E. Cholinesterase inhibitors: from the calabar bean to Alzheimer therapy. In *Cholinesterases and Cholinesterase inhibitors.* Giacobini, E., Ed.; Martin Dunitz: London, **2000**, pp. 181–226.
5. Viayna, E.; Sola, I.; Bartolini, M.; Simone. A. D.; Tapia-Rojas, C.; Serrano, F. G.; Sabate, R.; Juarez-Jimenez, J.; Perez, B.; Luque, F. J.; Andrisano, V.; Clos, M. V.; Inestrosa, N. C. and Munoz-Torrero, D. Synthesis and multitarget biological profiling oa a novel family of Rhein derivatives as disease-modifying anti-alzheimer agents. *J. Med. Chem.,* **2014**, *57*, 2549-2567.
6. Downes, G. B. and Granto, M. Acetylcholinesterase function is dispensable for sensary neurite growth but is critical for neuromuscular synapse stability. *Dev. Biol.,* **2004**, *270*, 232–245.
7. Silman, I. and Sussman, J. L. Acetylcholinesterase: Classical and non-classical functions and pharmacology. *Curr. Opin. Pharmacol.,* **2005**, *5*, 293-302.
8. Chubb, I. W.; Hodgson, A. J. and White, C. H. Acetylcholinesterase hydrolyses substance P. *Neuroscience,* **1980**, *5*, 2065-2072.
9. Chubb, I. W.; Ranieri, E.; Hodgson, A. J. and White, G. H. The hydrolysis of Leu and Met-enkephalin by acetylcholinesterase. *Neuroscilett. Suppl.,* **1982**, *8*, 539.
10. Lamers, W. H.; te Kartschot, A.; Los, J. A. and Moorman, A. F. Acetylcholinesterase in prenatal rat heart: a member for the early development of the cardiac conductive tissue? *Anat. Rec.,* **1987**, *217*, 361–370.
11. Lamers, W. H.; Geerts, W. J. and Moorman, A. F. Distribution pattern of acetylcholinesterase in early embryonic chicken hearts. *Anat. Rec.,* **1990**, *228*, 297–305.
12. Hawkins, R. D and Mendel, B. Selective inhibition of pseudo-cholinesterase by di*iso*propyl fluorophosphonate. *Brit. J. Pharmacol*., **1947**, *2*, 173-180.
13. Allderdice, P. W.; Gardner, H. A.; Galutira, D.; Lockridge, O.; LaDu, B. N. and McAlpine, P. J. "The cloned butyrylcholinesterase (BCHE) gene maps to a single chromosome site, 3q26". Genomics, **1991**, 11, 452–454.
14. Lenz, D. E.; Yeung, D.; Smith, J. R.; Sweeney, R. E.; Lumley, L. A. and Cerasoli, D. M. Stoichiometric and catalytic scavengers as protection against nerve agent toxicity: A mini review. *Toxicology,* **2007**, *233,* 31–39.
15. Geldenhuys, W. J. and Van der Schyf, C. J.; Rationally designed multitargeted agents against neurodegenerative diseases. *Curr. Med. Chem.,* **2013**, *20*, 1662-1672.
16. Xie, S,-S.; Wang, X.-B; Li, J.-Y.; Yang, L. and Kong, L.-Y. Design, synthesis and evaluation of novel tacrine-coumarin hybrids as multifunctional cholinesterase inhibitors against Alzheimer's disease. *Eur. J. Med. Chem.,* **2013**, *64*, 540-553.
17. Darvesh, S.; McDonald, R. S.; Darvesh, K. V.; Mataija, D.; Conrad, S.; Gomez, G.; Walsh, R. and Martin, E. Selective reversible inhibition of human butyrylcholinesterase by aryl amide derivatives of phenothiazine. *Bioorg. Med. Chem.,* **2007**, *15,* 6367–6378.
18. Nelson, T. C. and Burritt, M. F. Pesticide poisoning, succinylcholine-induced apnea, and pseudocholinesterase. *Mayo Clin Proc.*, **1986**, *61*, 750-752.
19. Finar, I.L., Organic Chemistry: Stereochemistry and the Chemistry of Natural Product, 5th ed.; Vol.2, pp. 621, **1975**.
20. Singhal, N.; Sharma, P. K.; Dudhe, R. and Kumar, N. Recent advancement of triazole derivatives and their biological significance. *J. Chem. Pharm. Res.,* **2011**, *3*, 126-133.
21. Smith, G. S.; Kramer, E.; Ma, Y.; Hermann, C. R.; Dhawan, V.; Chaly, T. and Eidelberg, D. Cholinergic modulation of the cerebral metabolic response to citalopram in Alzheimer's disease. *Brain*., **2009**, *132*, 392–401.
22. Walsh, R.; Rockwood, K.; Martin, E. and Darvesh, S. Synergistic inhibition of butyrylcholinesterase by galantamine and citalopram. *Biochim. Biophys. Acta*., **2012**, *1810*, 1230-1235.
23. Kumar, R.; Yar, M. S.; Chaturvedi, S. and Srivastava, A. Triazole as pharmaceuticals potentials. *Int. J. PharmTech. Res.,* **2013**, *5*, 1844-1869.
24. Furniss, B. S.; Rogers, V.; Smith, P. W. G. and Tatchell, A. R. *Vogel's textbook of practical organic chemistry,* 5th ed.; Longman Scientific and Technical: Essex England, pp. 1342-1349, **1989**.
25. Kap-Sun, Y.; Michelle, E. F.; John, F. K. and Nicholas, A. M. A base catalyzed, direct synthesis of 3,5-disubstituted 1,2,4-triazoles from nitriles and hydrazides. *Tetrahedron Lett.,* **2005**, *46,* 3429-3432.
26. Mohite, P. B.; Pandhare, R. B.; Khanage, S. G. and Bhaskar, V. H. A novel approach for synthesis of substituted tetrazoles. *Dig. J. Nanomater. Bios.*, **2009**, *4,* 803–807.
27. Saxena, A.; Redman, A. M. G.; Jiang, X.; Lockridge, O. and Doctor, B. P. D., Differences in active site gorge dimensions of cholinesterases revealed by binding of inhibitors to human butyrylcholinesterase. *Biochemistry,* **1997**, *36*, 14642-14651.
28. Savini, L.; Gaeta, A.; Fattorusso, C.; Catalanotti, B.; Campiani, G.; Chiasserini, L.; Pellerano, C.; Novellino, E.; McKissic, D. and Saxena, A. Specific targeting of acetylcholinesterase and butyrylcholinesterase recognition sites. Rational design of novel, selective, and highly potent cholinesterase inhibitors. *J. Med. Chem.,* **2003**, *46*, 1-4.
29. Sussman, J. L.; Harel, M.; Frolow, F.; Oefner, C.; Goldman, A.; Toker, L. and Silman, I. Atomic structure of acetylcholinesterase from Torpedo californica: a prototypic acetylcholine-binding protein. *Science,* **1991**, *253*, 872-879.
30. Cheung, J.; Gary, E. N.; Shiomi, K. and Rosenberry, T. L. Structures of human acetylcholinesterase bound to dihydrotanshinone I and territrem B show peripheral site flexibility. *Med. Chem. Lett.,* **2013**, *4,* 1091-1096.
31. Nachon, F.; Carletti, E.; Ronco, C.; Trovaslet, M.; Nicolet, Y.; Jean, L. and Renard, P. Y. Crystal structures of human cholinesterases in complex with huprine W and tacrine: elements of specificity for anti-Alzheimer's drugs targeting acetyl- and butyrylcholinesterase. *Biochem. J.,* **2013**, *453*, 393-399.
32. Labute, P. The generalized Born/volume integral implicit solvent model: estimation of the free energy of hydration using London dispersion instead of atomic surface area. *J. Comput. Chem.*, **2008**, *29*, 1693-1698.
33. Saha, A.; Kumar, R.; Kumar, R. and Devakumar, C. Development and assessment of green synthesis of hydrazides. *Indian J. Chem. B,* **2010**, *49*, 526-531.
34. Sammaiah, G.; Brahmeshwari, G. and Sarangapani, M. Synthesis and biological activity of 2-aminobenzoic acid (2-oxo-1,2-dihydro-indol-3-ylidene)-hydrazides. *J. Adv. Pharmaceut. Sci. (India),* **2011**, *1*, 111-121.
35. Haider, A.; Akhter, Z.; Siddiqi, H. M. and Tiekink, E. R. T. Crystal and molecular structure of 4-aminobenzohydrazide. *J. Chem. Crystallogr.*, **2010**, *40*, 397-401.
36. www.alfa.com/en/catalog/
(a) A11491, (b) L04357, (c) B21330, (d) B20800, (e) A180186, (f) L00937, (g) A19628, (h) A18918, (i) A13619, (j) B20956
37. Zaheer, M.; Zia-ur-Rehman, M.; Rahman, S.; Ahmed, N. and Chaudhary, M. I. Microwave assisted synthesis of biologically active 4-hydroxy-*N*-(phenylcarbonyl)-2H-1,2-benzothiazine-3-carbohydrazide-1,1-dioxide derivatives. *J. Chil. Chem. Soc.,* **2012**, *57*, 1492-1496.
38. Bhole, R. P.; Borkar, D. D.; Bhusari, K. P. and Patil, P. A. Design and synthesis of *p*-hydroxybenzohydrazide derivatives for their

antimycobacterial Activity. *J. Korean Chem. Soc.,* **2012**, *56*, 236-245.
39. Ahmad, S.; Jabbar, A.; Hussain, M. T. and Tahir, M. N. 2-Chlorobenzohydrazide. *Acta Cryst.,* **2012**, *E68*, o1254.
40. Harer, S. L.; Rajurkar, V. G.; Patil, P.; Harer, P. S.; Navale, S. D.; Awuti, S. T. and Sonawane, A. A. Synthesis, characterization and anti-microbial evaluation of some 2-iodo-*N*'-[(1*E*)-substituted phenylmethylidene]benzohydrazide analogues. *Int. J. Pharma. Sci. Drug Res.,* **2010**, *2*, 134-136.
41. www.matrixscientific.com/006684.html
42. Wild, F. *Characterization of organic compounds.* 2nd ed.; Cambridge University Press: UK, pp.119, **1958**.
43. Toda, F.; Hyoda, S. Okada, K. and Hirotsu, K. Isolation of anhydrous hydrazine as stable inclusion complexes with hydroquinone and *p*-methoxyphenol, and their solid state reaction with esters which gives pure hydrazides. *J. Chem. Soc. Chem. Commun.,* **1995**, *15,* 1531-1532.
44. Ellman, G. L.; Courtney, K. D.; Andres, V. and Featherstone, R. M. A new and rapid colorimetric determination of acetylcholinesterase activity. *Biochemical. Pharmacology.,* **1961**, *7*, 88-95.